Int. J. Morphol.,
44(1):9-22, 2026.

Effects of Maternal Separation on Lipid Homeostasis and Visceral Adipose Tissue Organization in Mice Fed a High-fat Diet Post-weaning

Efectos de la Separación Materna Sobre la Homeostasis Lipídica y La Organización del Tejido Adiposo Visceral en Ratones Alimentados con Dieta Alta en Grasas Post-destete

Javiera Navarrete[1] & Bélgica Vásquez[1,2,3]

NAVARRETE, J. & VÁSQUEZ, B. Effects of maternal separation on lipid homeostasis and visceral adipose tissue organization in mice fed a high-fat diet post-weaning. *Int. J. Morphol., 44(1)*:9-22, 2026.

SUMMARY: Early-life stress and obesity represent critical public health challenges. This study investigated the effects of maternal separation (MS), as a model of early-life adversity, and post-weaning high-fat diet (HFD) exposure on plasma lipid profile and visceral adipose tissue organization in C57BL/6 male mice. Mice underwent MS during the early postnatal period or were left unmanipulated (UM). Following weaning, animals were allocated to a control diet (CD) or an HFD, yielding four experimental groups (n = 5 per group): UM-CD, MS-CD, UM-HFD, and MS-HFD. Plasma lipid profile, global adiposity index, and the mass of perigonadal (PGAT), retroperitoneal (RPAT), and mesenteric (MSAT) visceral adipose tissue deposits, as well the histological architecture and sectional area (SA) of adipocytes, were evaluated using morphological and quantitative analyses. HFD was the primary determinant of alterations in the plasma lipid profile, particularly total cholesterol (CHOL-T) and low-density lipoprotein cholesterol (LDL-C), whereas MS selectively modulated the magnitude of these changes. The global adipocity index was predominantly influenced by dietary intervention, with no significant effect of MS. In contrast, visceral fat pad expansion was heterogeneous and depot-specific, with a significant diet × MS interaction detected in RPAT and, to a lesser extent, in MSAT. Histological and quantitative analyses showed that HFD induced a significant increase in SA in all three visceral fat pads, with MS contributing in a depot-dependent manner, revealing non-uniform patterns of adipose tissue expansion. In conclusion, these findings indicate that MS does not act as a direct determinant of obesity, but rather as a programming factor that modulates the plasma lipid profile and the structural response of visceral adipose tissue to an obesogenic nutritional environment in adulthood.

KEY WORDS: Maternal separation; High-fat diet; Lipid profile; Visceral adipose tissue; Mouse.

INTRODUCTION

Obesity and metabolic syndrome currently constitute major public health challenges worldwide. Their prevalence has steadily increased over recent decades, affecting both adult and pediatric populations. This trend is associated with a substantial rise in chronic non-communicable diseases, including type 2 diabetes mellitus, cardiovascular disease, dyslipidemia, and premature mortality. Consequently, obesity imposes a significant global health and economic burden (Saklayen, 2018; Di Cesare *et al*., 2019). In this context, obesity is no longer considered merely an excess accumulation of body fat but rather is recognized as a complex disease characterized by profound metabolic and systemic dysfunction.

The paradigm shift in understanding adipose tissue has been fundamental in explaining the metabolic consequences of obesity. Adipose tissue is now recognized as a highly active endocrine and immunometabolic organ that secretes a broad spectrum of adipokines, cytokines, and other bioactive factors, which regulate metabolic, inflammatory, and hormonal processes at the systemic level (Kwon *et al*., 2013; Kirichenko *et al*., 2022; Radzik-Zajac *et al*., 2023). In obesity, the expansion of adipose tissue, mainly through adipocyte hypertrophy, is associated with low-grade chronic inflammation, infiltration of immune cells, insulin resistance, and alterations in lipid metabolism. All these factors contribute to the development of metabolic

[1] Doctoral Program in Morphological Sciences, Faculty of Medicine, Universidad de La Frontera, Temuco, Chile.
[2] Center of Excellence in Morphological and Surgical Studies, Universidad de La Frontera, Temuco, Chile.
[3] Department of Basic Sciences, Faculty of Medicine, Universidad de La Frontera, Temuco, Chile.
FUNDING: This research was funded by the University of La Frontera, project DIUFRO DI24-0029.

Received: 2025-12-19 Accepted: 2026-01-07

syndrome and related diseases (Guzik *et al*., 2017; Zatterale *et al*., 2020).

In parallel, increasing evidence suggests that susceptibility to obesity and metabolic dysfunction is determined not only by genetic factors or adult lifestyle, but may also originate during the early stages of development. The Developmental Origins of Health and Disease (DOHaD) paradigm posits that environmental exposures during critical windows of prenatal and postnatal development can permanently program the structure and function of organs and systems, thereby influencing disease risk in adulthood (Gluckman, 2005; Vickers, 2014). These early-life adaptations, referred to as predictive adaptive responses, may be advantageous in matching environments but confer metabolic vulnerability when there is a mismatch between early and later life conditions (López *et al*., 2023).

Within this framework, early postnatal life emerges as a particularly sensitive and critical window for metabolic programming. During this stage, metabolically active tissues such as the liver, pancreas, skeletal muscle, and adipose tissue display marked structural and functional plasticity, rendering them highly susceptible to environmental influences including stress and nutritional factors (Barouki *et al*., 2012; Sheng *et al*., 2021). Specifically, regarding adipose tissue, the postnatal period is characterized by robust proliferation and differentiation of adipocyte precursors, particularly within visceral fat pads, which substantially determines the capacity for adipose expansion and metabolic function in adulthood (Holtrup *et al*., 2017).

Early-life stress is a highly significant non-nutritional factor in the developmental programming of physiological systems. Among the most extensively characterized experimental models for investigating its effects is maternal separation (MS), a rigorously validated paradigm that mimics early-life adversity during critical windows of postnatal neurodevelopment (Zimmerberg *et al*., 2011; Daskalakis *et al*., 2012). Prolonged exposure to MS disrupts the stress hyporesponsive period (SHRP), inducing persistent alterations in the regulation of the hypothalamic-pituitary-adrenal (HPA) axis, including sustained elevations in glucocorticoid secretion and heightened stress responsivity in adulthood (Nishi *et al*., 2020).

These neuroendocrine alterations induced by early-life stress have profound metabolic consequences. Numerous studies have demonstrated that animals exposed to MS display persistent disruptions in feeding behavior, heightened preference for energy-dense palatable foods, increased visceral adiposity, dyslipidemia, and impaired insulin sensitivity, even in the absence of additional dietary stressors (Silva *et al*., 2013; Vargas *et al*., 2016). Moreover, MS has been linked to both structural and functional remodeling in peripheral organs, such as the liver, further supporting the role of early-life programming in shaping tissue architecture and metabolic health (del Sol *et al*., 2025).

The consequences of early-life programming factors frequently become more pronounced upon subsequent exposure to a secondary metabolic insult. Within this framework, the double-hit hypothesis suggests that an initial adverse event induces a latent susceptibility, which is unmasked only following a second challenge, such as consumption of an obesogenic diet (López-Taboada *et al*., 2024). Post-weaning exposure to a high-fat diet (HFD) constitutes a particularly salient metabolic stressor, as the post-weaning period is a critical window for the establishment of energy homeostasis and adipose tissue expansion (Yang *et al*., 2022; Sakers *et al*., 2022).

Post-weaning exposure to HFDs induces adipocyte hypertrophy, dysregulation of adipokine secretion, chronic low-grade inflammation in adipose tissue, and systemic metabolic derangements, outcomes that frequently persist into adulthood (Choe *et al*., 2016; Rodríguez-González *et al*., 2023). Notably, the combination of this nutritional challenge with antecedent early-life stress synergistically exacerbates alterations in adipose tissue biology and metabolic function, resulting in more pronounced obesogenic phenotypes than those elicited by either factor alone (Tamashiro *et al*., 2009; Leachman *et al*., 2022).

Despite robust evidence regarding the independent effects of early-life stress and obesogenic diets, critical gaps persist in elucidating the mechanisms by which these exposures interact to durably program adipose tissue organization. Specifically, limited data exist on how early MS influences cellular architecture, adipogenic potential, and the regional distribution of visceral adipose fat pads in response to subsequent nutritional insults. Addressing this interplay is essential for delineating the early-life determinants of differential susceptibility to obesity and metabolic disorders in adulthood. Accordingly, the objective of this study was to assess the impact of early-life MS on plasma lipid profiles and the structural organization of visceral adipose tissue in mice subjected to post-weaning HFD exposure.

MATERIAL AND METHOD

Animals

This study utilized adipose tissue samples derived from an established experimental model conducted under the auspices of the UFRO-DIUFRO project (code DI24-

0029), designed to evaluate the impact of MS and post-weaning HFD exposure on pancreatic morphology and function in male C57BL/6 mice. Leveraging the same cohort enabled comprehensive analysis of additional metabolically relevant tissues, thereby minimizing animal usage in accordance with the principles of reduction and refinement articulated in the 3Rs (Russell & Burch, 1959).

All experimental procedures adhered to the Guide for the Care and Use of Laboratory Animals (Institute for Laboratory Animal Research, 2011). The overarching protocol received approval from the Scientific Ethics Committee of the University of La Frontera (File Number 067_24, May 28, 2024), explicitly authorizing the collection and analysis of supplementary tissue and plasma samples. Subsequent analyses focused on adipose tissue and plasma were separately reviewed and approved by the same ethics committee (File Number 116_24, September 3, 2024).

Female C57BL/6 mice were procured from the Animal Facility of the Center of Excellence in Morphological and Surgical Studies (CEMyQ), University of La Frontera, Chile. Animals were housed under controlled environmental conditions (temperature and humidity), maintained on a 12:12 h light-dark cycle, with ad libitum access to standard chow and water. Sexually mature, nulliparous females were co-housed with males overnight, and successful mating was verified by the presence of vaginal plugs. Pregnant females were subsequently housed individually. Throughout gestation and lactation, dams were provided a purified control diet (CD; AIN-93G), as recommended by the American Institute of Nutrition for optimal support of gestation, lactation, and postnatal growth (Reeves *et al*., 1993) (Table I). Diets were formulated by PRAGSOLUÇÕES Biociências (www.pragsolucoes.com.br) and stored at -20 °C for the duration of the study to ensure preservation of nutritional integrity.

Table I. Composition of experimental diets administered in the study. Animals were provided either a control diet (CD) or a high-fat diet (HFD). Vitamin and mineral mixes were formulated according to AIN-93G guidelines for laboratory rodents. The HFD delivered 49% of total caloric intake from lipids.

Ingredients	CD	HFD
Casein (> 85 % protein)	200.0	230.0
L-cystine (g/kg)	3.0	3.0
Cornstarch (g/kg)	529.486	299.472
Sucrosa (g/kg)	100.0	100.0
Soybean oil (g/kg)	70.0	70.0
Lard (g/kg)	-	200.0
Fiber (g/kg)	50.0	50.0
Vitamin mixture (g/kg)[1]	10.0	10.0
Mineral mixture (g/kg)	35.0	35.0
Choline bitartrate (g/kg)	2.5	2.5
Antioxidant (g/kg)	0.014	0.028
Total (g)	1000.0	1000.0
Energy (kcal/g)	3.95	4.95
Carbohydrate (% Energy)	64.0	32.0
Protein (% Energy)	19.0	19.0
Lipid (% Energy)	17.0	49.0

[1] whitout vitamin D.

Beginning three days prior to the anticipated parturition date, dams were monitored twice daily (at the onset and conclusion of the light phase) for the presence of pups. The day of birth was designated as postnatal day 0 (PND 0). Sex determination was conducted on postnatal day 2 (PND 2) by visual inspection for a darkly pigmented spot in the anogenital region, a marker specific to male neonates bearing dark pigmentation. This approach enabled accurate and early sex differentiation, as female pups lack this characteristic (Wolterink-Donselaar *et al*., 2009). To standardize nutritional access during lactation, litter sizes were randomly adjusted to seven pups per dam.

Maternal separation

Following litter standardization, pups were randomly allocated to one of two experimental groups: the unmanipulated (UM) cohort, in which offspring remained with their dams until conventional weaning at postnatal day 21 (PND 21), and the MS cohort, subjected to extended daily separation periods in conjunction with early weaning.

The MS protocol followed the guidelines described by George *et al*. (2010): pups underwent 240 minutes of daily separation from postnatal day 2 (PND 2) to PND 5, followed by 480 minutes daily from PND 6 to PND 16, and were weaned prematurely at PND 17. During separation epochs, pups were maintained in their home cage on a thermostatically controlled heating pad (32 - 34 °C) to ensure adequate thermoregulation, while dams were housed in separate cages within the same facility under identical environmental conditions, with unrestricted access to food and water. Daily monitoring was conducted to assess for clinical signs of dehydration or distress, in accordance with the "Animal Supervision" protocol outlined by Morton & Griffiths (1985). In both groups, all husbandry procedures, including routine cage maintenance, were conducted by a single operator to minimize confounding stressors.

Post-weaning diet

At weaning (PND 21 for the UM group and PND 17 for the MS group), a single male pup from each litter was randomly selected to establish four experimental cohorts (n

= 5 per group; total n = 20), based on dietary intervention: control diet (CD) or high-fat diet (HFD). The resulting groups were as follows: UM-CD (unmanipulated, control diet), MS-CD (maternal separation, control diet), UM-HFD (unmanipulated, high-fat diet) and MS-HFD (maternal separation, high-fat diet) (Fig. 1). Only male offspring were included to minimize variability associated with estrous cycle effects on anxiety-related behaviors and energy intake (Rees *et al*., 2008). Mice were maintained on their respective diets for 16 weeks, as specified in Table I (Aguila *et al*., 2021).

In accordance with established morphological methodologies and the 3R principles of reduction and refinement (Russell & Burch, 1959), five animals were included per experimental group. This sample size was methodologically adequate to detect meaningful morphological trends. As described by Cruz-Orive & Weibel (1990), achieving consistent findings from a cohort of this size corresponds to a probability of random error of $P = (1/2)^5 = 0.03125$, thereby supporting the validity of results within the context of an exploratory investigation.

Euthanasia

Upon completion of the 16-week post-weaning intervention, and following a six-hour fasting period, body mass was measured for each animal. Euthanasia was subsequently conducted via overdose of ketamine/xylazine (240/30 mg/kg), in accordance with the ethical standards established by the Canadian Council on Animal Care (1993). After confirmation of deep anesthesia, whole blood was collected by direct left ventricular cardiac puncture. Blood samples were transferred to EDTA-coated tubes and centrifuged immediately at 3000 rpm for 15 min at 4°C to isolate plasma. Plasma aliquots were stored at -80°C pending biochemical analyses.

Following blood collection, perigonadal (PGAT), retroperitoneal (RPAT), and mesenteric (MSAT) adipose tissue deposits were meticulously excised. Both total body mass and individual fat pad mass were determined using an analytical balance (A&D Orion® HR 120, A&D Technology, Saitama, Japan). The global adiposity index was subsequently calculated as the percentage of total fat pad mass relative to body mass.

Plasma lipid profile

Plasma concentrations of total cholesterol (CHOL-T), triglycerides (TG), low-density lipoprotein cholesterol (LDL-C), and high-density lipoprotein cholesterol (HDL-C) were quantified using a kinetic colorimetric assay with commercially available kits (Wiener Lab., Rosario, Argentina).

Histological processing and staining

Adipose tissue fat pads were immersed in fixative (1.27 mol/L formaldehyde in 0.1 M phosphate buffer, pH 7.2) for 48 h at room temperature. Samples were subsequently dehydrated in graded ethanol, cleared in xylene, and embedded in Paraplast Plus (Sigma-Aldrich Co., St. Louis, MO, USA). Owing to their small size, the entire fat pads were embedded intact. Serial sections of 4 µm thickness were obtained using a microtome (Leica® RM2255, Leica Biosystems, Deer Park, IL, USA).

For histological and quantitative analyses of adipose tissue, ten sections per sample, separated by 150 µm, were stained with hematoxylin and eosin (H&E). Histological images were acquired using a Leica® DM750 microscope (Leica Microsystems, Heerbrugg, Switzerland) equipped with a Leica® ICC50 HD digital camera (Leica

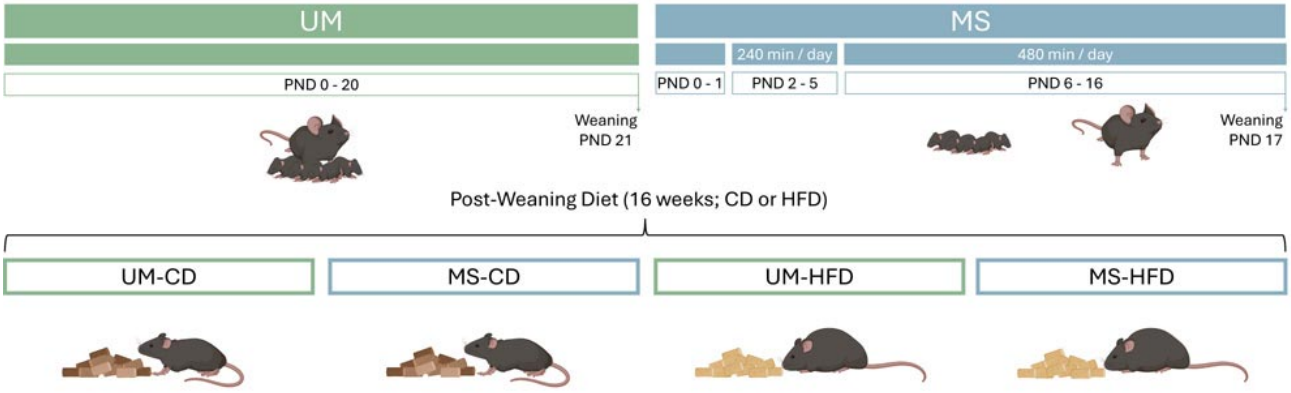

Fig. 1. Experimental design of maternal separation and post-weaning dietary intervention. Schematic representation of the experimental timeline and group allocation. PND: postnatal day; UM: unmanipulated; MS: maternal separation; CD: control diet; HFD: high-fat diet; UM-CD: unmanipulated, control diet; MS-CD: maternal separation, control diet; UM-HFD: unmanipulated, high-fat diet; MS-HFD: maternal separation, high-fat diet.

Microsystems, Heerbrugg, Switzerland) and visualized on a ViewSonic® LCD monitor (ViewSonic Corporation, Brea, CA, USA).

Sectional area of adipocytes

For morphometric analysis of adipocytes, the mean sectional area (SA) was estimated using the formula $SA = V_V / 2 \times (N/A_T)$, where V_V represents volume density, N is the number of adipocyte profiles counted, and A_T denotes the test area. This stereological approach minimizes bias associated with direct diameter measurements by employing probabilistic and statistical principles (Mandarim-de-Lacerda & del Sol, 2017).

Randomly selected microscopic fields were analyzed until a minimum of 200 adipocytes per mouse (approximately five fields per animal) were assessed, a sample size deemed sufficient for statistical accuracy in stereological studies (Gundersen *et al*., 1999; Slomianka & West, 2005). Slides were examined using a Leica® DM2000 LED stereological microscope (Leica Microsystems, Heerbrugg, Switzerland) and imaged with a Leica® MC170 HD digital camera (Leica Microsystems, Heerbrugg, Switzerland). The 36-point grid system implemented with STEPanizer® software (version 2.28, https://www.stepanizer.com) was utilized to determine volume density (V_V) by quantifying points intersecting adipocytes (P_p) relative to the total grid points (P_T), calculated as $V_V = P_p/P_T$ (%). Adipocyte mass was then calculated by multiplying V_V by the mass of the respective fat pad.

Statistical Analysis

Data distribution was evaluated using the Shapiro-Wilk test for normality and Levene's test for homogeneity of variances. For lipid profile variables that did not meet normality assumptions, group differences were assessed with the Kruskal-Wallis test, followed by *post hoc* pairwise comparisons using Dunn's test with Bonferroni correction. Robust ANOVA was additionally employed to validate the consistency of results and to identify potential violations of parametric assumptions. For adipose tissue-related variables (global adiposity index, fat pad mass, mean adipocyte sectional area [SA]), a two-way ANOVA was used, with MS and diet as factors and their interaction (diet × MS) as factors. Linear regression and correlation analyses were performed to examine associations among continuous variables. Statistical significance was set at $p < 0.05$. Data analyses were performed using GraphPad Prism v10.6.1 (GraphPad Software, Boston, MA, USA), and robust ANOVA was conducted in jamovi v2.6.44 (The jamovi project).

RESULTS

Plasma lipid profile

Analysis of the plasma lipid profile revealed that the various parameters responded differently to the post-weaning diet and to MS, displaying specific patterns depending on the lipid fraction assessed (Table II).

CHOL-T exhibited significant differences among the experimental groups. Increases were observed in association with both HFD and MS, with particularly elevated values when both factors were combined. Nonparametric analysis confirmed overall differences between groups, while a robust factorial analysis demonstrated significant main effects of both diet and MS, with no interaction between the two factors.

Table II. Plasma lipid profile of male C57BL/6 mice subjected to maternal separation and post-weaning high-fat diet exposure.

	Median (Q1–Q3)				Kruskal Wallis	Robust two-way ANOVA (trimmed means)		
mg/dl	**UM-CD**	**MS-CD**	**UM-HFD**	**MS-HFD**	***p*-Value**	**Diet**	**MS**	**Interaction**
CHOL-T	43 (39–55)	98 (92.5–99.3)[a]	83 (77–88.5)	151.8 (110–202.5)[c]	0.0005	Q = 9.5, p = < 0.037	Q = 18.4, p = < 0.010	ns
TG	84 (63–141)	60.3 (36.5–103.15)	33 (16.5–69.5)	62 (39.5–111)	0.1741	ns	ns	ns
LDL-C	13.8 (12.75–16.7)	17.8 (14.1–31.2)	44.1 (23.75–59.1)	98.6 (76.1–147.15)[c]	0.0015	Q = 54.8, p = 0.001	Q = 16.1, p = 0.006	Q = 11.2, p = 0.016
HDL-C	25.5 (25.5–51)	71.4 (48.15–73.95)	30.6 (20.4–45.9)	31.8 (20.4–43.35)	0.0593	Q = 6.9, p = 0.036	Q = 8.9, p = 0.021	Q = 10.2, p = 0.015

Group-wise data are shown as median (interquartile range, Q1–Q3) and were compared using the Kruskal–Wallis test with adjusted post hoc analyses. Factorial effects of diet and maternal separation were assessed using robust two-way ANOVA based on trimmed means. UM-CD: unmanipulated, control diet, MS-CD: maternal separation control diet, UM-HFD: unmanipulated, high-fat diet, MS-HFD: maternal separation, high-fat diet. [a] Statistically significant ($p < 0.05$) with the UM-CD group, [b] Statistically significant ($p < 0.05$) with the MS-CD group, [c] Statistically significant ($p < 0.05$) with the UM-HFD group.

LDL-C displayed a marked response pattern, with significant differences among the experimental groups. HFD was associated with a pronounced increase in plasma LDL-C levels, an effect significantly modulated by MS. Robust factorial analysis identified significant main effects of both diet and MS, as well as a significant interaction between these factors, indicating that the combination of HFD and MS amplified the increase in this lipid fraction.

For HDL-C, no significant overall differences were detected among groups in the nonparametric analysis. However, robust factorial analysis revealed significant effects of both diet and MS, as well as their interaction, suggesting a context-dependent response and more complex regulation of this lipid fraction compared to CHOL-T and LDL-C.

Global adiposity index

The global adiposity index exhibited a response pattern clearly determined by diet type (Fig. 2). Animals fed CD displayed low and homogeneous values, with no differences attributable to MS. In contrast, HFD induced a pronounced increase in the global adiposity index in both unmanipulated animals and those subjected to MS, although no significant differences were observed between these groups within the same diet.

Two-way ANOVA analysis confirmed that diet was the main determinant of the overall global adiposity index, explaining 77.9 % of the total observed variation ($F = 76.19$; $p < 0.0001$). MS contributed marginally (2.99 %; $F = 2.93$; $p = 0.11$), and no significant interaction between the two factors was detected.

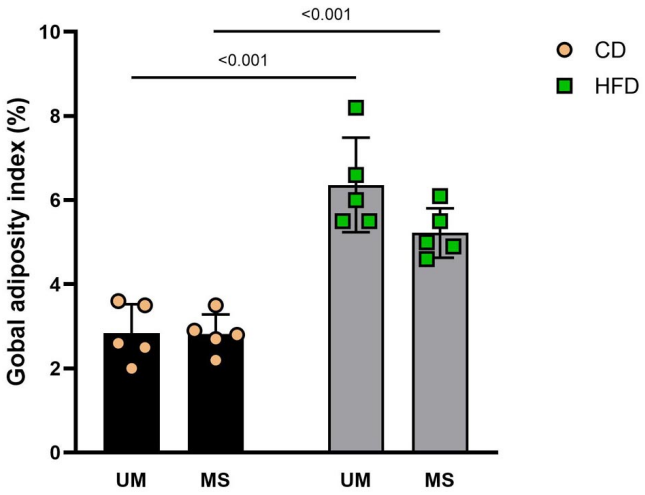

Fig. 2. Global adiposity index according to dietary intervention and maternal separation. UM: unmanipulated; MS: maternal separation; CD: control diet; HFD: high-fat diet. Bar graphs depict mean ± SD; dots indicate individual animals.

Mass of fat pads

Analysis of adipose pad mass revealed site-specific responses, with diet as the predominant determinant and MS variably modulating these effects (Fig. 3, Table III).

In PGAT, exposure to a HFD resulted in a significant increase in fat pad mass, particularly in the UM-HFD group. Two-way ANOVA demonstrated a highly significant main effect of diet ($p < 0.0001$), accounting for 67.8 % of the total variance, with no significant effects of MS or diet × MS interaction (Fig. 3, Table III).

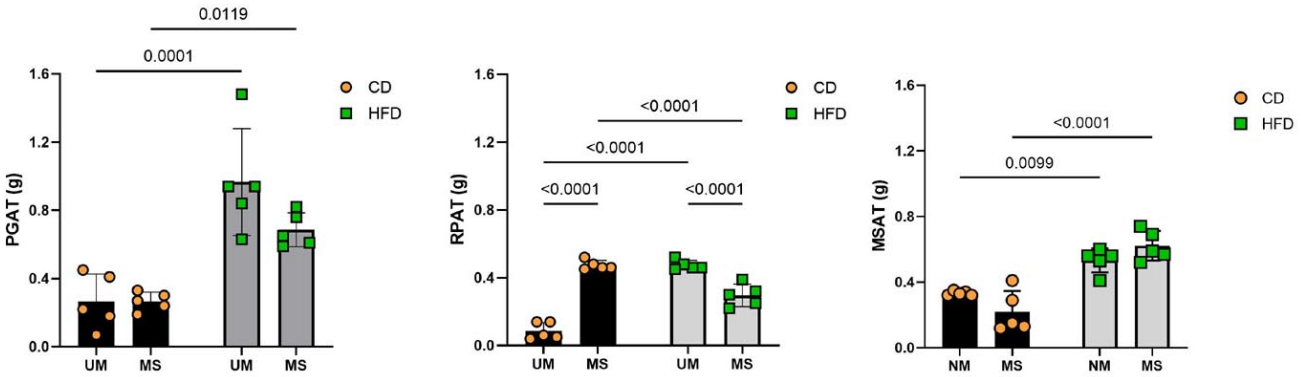

Fig. 3. Absolute mass of perigonadal (PGAT), retroperitoneal (RPAT), and mesenteric (MSAT) adipose tissue deposits in male C57BL/6 mice subjected to maternal separation and post-weaning high-fat diet exposure. UM: unmanipulated group; MS: maternal separation group; CD: control diet; HFD: high-fat diet. Bar graphs depict mean ± SD; dots indicate individual animals. Statistically significant differences between groups are indicated in each panel ($p < 0.05$).

Table III. Two-way ANOVA assessing the relative contribution of post-weaning diet, maternal separation (MS), and their interaction (diet × MS) to the variance in fat pad mass in male C57BL/6 mice.

Data	Variation and significance test					
	Diet effect		MS effect		Diet x MS	
	%	*p*	%	*p*	%	*p*
PGAT	67.8	< 0.0001	4.2	ns	4.2	ns
RPAT	10.1	0.0001	10.1	0.0001	73.6	< 0.0001
MSAT	72.7	< 0.0001	0.1	ns	8.2	0.0184

Perigonadal (PGAT), retroperitoneal (RPAT) and mesenteric (MSAT) adipose tissue deposits. Data represent the percentage of variance explained (%) and the associated p values for each main factor and their interaction. ns: not significant; $p < 0.05$ considered statistically significant.

In RPAT, the response was more pronounced and dependent on the interaction of experimental factors. HFD exposure induced a significant increase in fat pad mass, but this effect was strongly modulated by MS. Statistical analysis revealed a highly significant diet × MS interaction ($p < 0.0001$), accounting for 73.6 % of the total variance, in addition to significant main effects of both factors. These findings indicate that the RPAT response to dietary challenge is heterogeneous and contingent on early-life history.

In MSAT, diet was also the principal factor associated with increased fat pad mass, although the response pattern was more heterogeneous. Significant increases were observed in the HFD groups, particularly among animals exposed to MS. Two-way ANOVA confirmed a significant main effect of diet ($p < 0.0001$) and a significant diet × MS interaction ($p = 0.0184$), whereas MS alone did not exert a significant effect. These differences in adipose pad mass were also evident macroscopically, with clear variations in tissue size and appearance across diets and MS (Fig. 4).

The mass of the different adipose pads increased proportionally with body mass, with significant positive associations observed for PGAT, RPAT, and MSAT (Fig. 5). Linear regression analysis demonstrated comparable slopes among the pads, indicating a similar rate of adipose tissue expansion relative to body mass. However, significant differences in intercepts ($p < 0.001$) indicated differences in baseline mass among the adipose pads.

Since the increase in the mass of the different adipose pads was closely associated with the increase in body mass (Fig. 5), we evaluated whether this growth occurred in a coordinated manner across the different adipose compartments. As the pads were obtained from the same animals, the associations between their masses were analyzed using correlation analysis to identify patterns of joint expansion among PGAT, RPAT, and MSAT (Table IV).

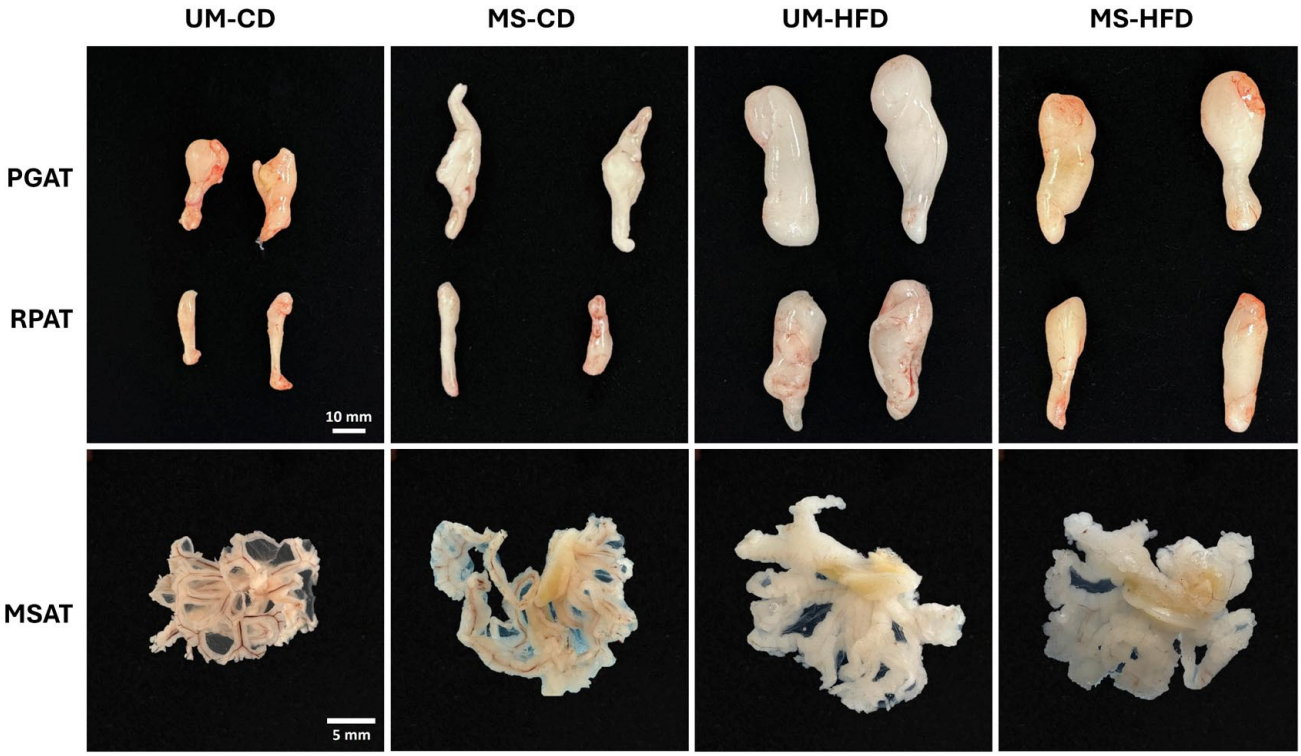

Fig. 4. Macroscopic morphology of the perigonadal (PGAT), retroperitoneal (RPAT), and mesenteric (MSAT) adipose tissue deposits from male C57BL/6 mice subjected to maternal separation and post-weaning high-fat diet exposure. UM-CD: unmanipulated, control diet; MS-CD: maternal separation, control diet; UM-HFD: unmanipulated, high-fat diet; MS-HFD: maternal separation, high-fat diet.

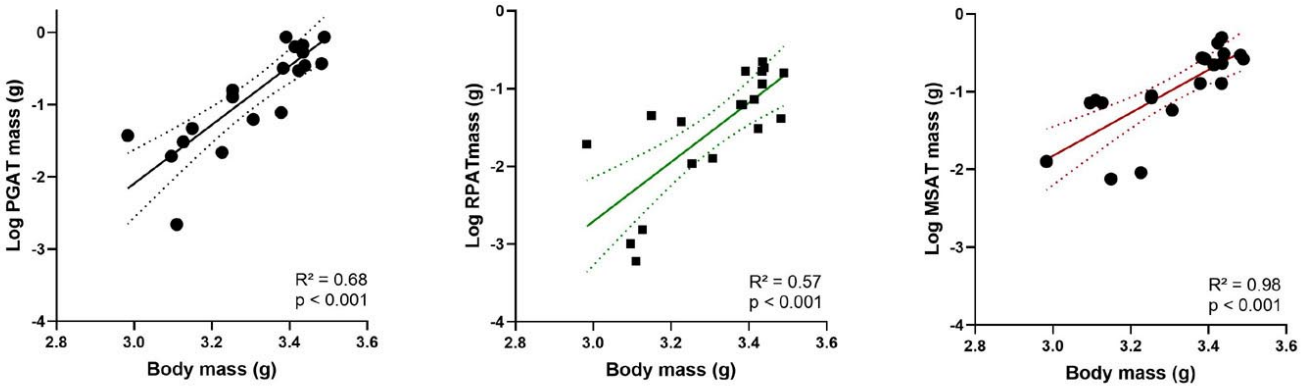

Fig. 5. Linear regression analysis of body mass *versus* total fat pad mass in male C57BL/6 mice subjected to maternal separation and post-weaning high-fat diet exposure. Perigonadal (PGAT), retroperitoneal (RPAT) and mesenteric (MSAT) adipose tissue deposits. Scatter plots depict individual animals, and solid lines indicate fitted linear regression models with 95 % confidence intervals. Analyses were conducted using log-transformed data. Coefficients of determination (R^2) and p-values are indicated in each panel.

Table IV. Spearman's correlation analysis of perigonadal (PGAT), retroperitoneal (RPAT), and mesenteric (MSAT) adipose tissue deposits mass in male C57BL/6 mice subjected to maternal separation and post-weaning high-fat diet exposure.

Variable 1	Variable 2	ρ (Spearman)	p value	n
PGAT	RPAT	0.8415	< 0.0001	20
PGAT	MSAT	0.7154	0.0004	20
RPAT	MSAT	0.5618	0.0099	20

Data are presented as Spearman's correlation coefficient (ρ), corresponding p values, and sample size (n). $p < 0.05$ considered statistically significant.

Histological analysis of adipose tissue

Representative histological sections of PGAT, RPAT, and MSAT displayed the characteristic architecture of white adipose tissue, composed of large unilocular adipocytes. The adipocytes exhibited predominantly rounded or polygonal contours, with flattened nuclei displaced toward the cell periphery when intersected by the section plane; this general morphology was preserved across all experimental groups (Fig. 6).

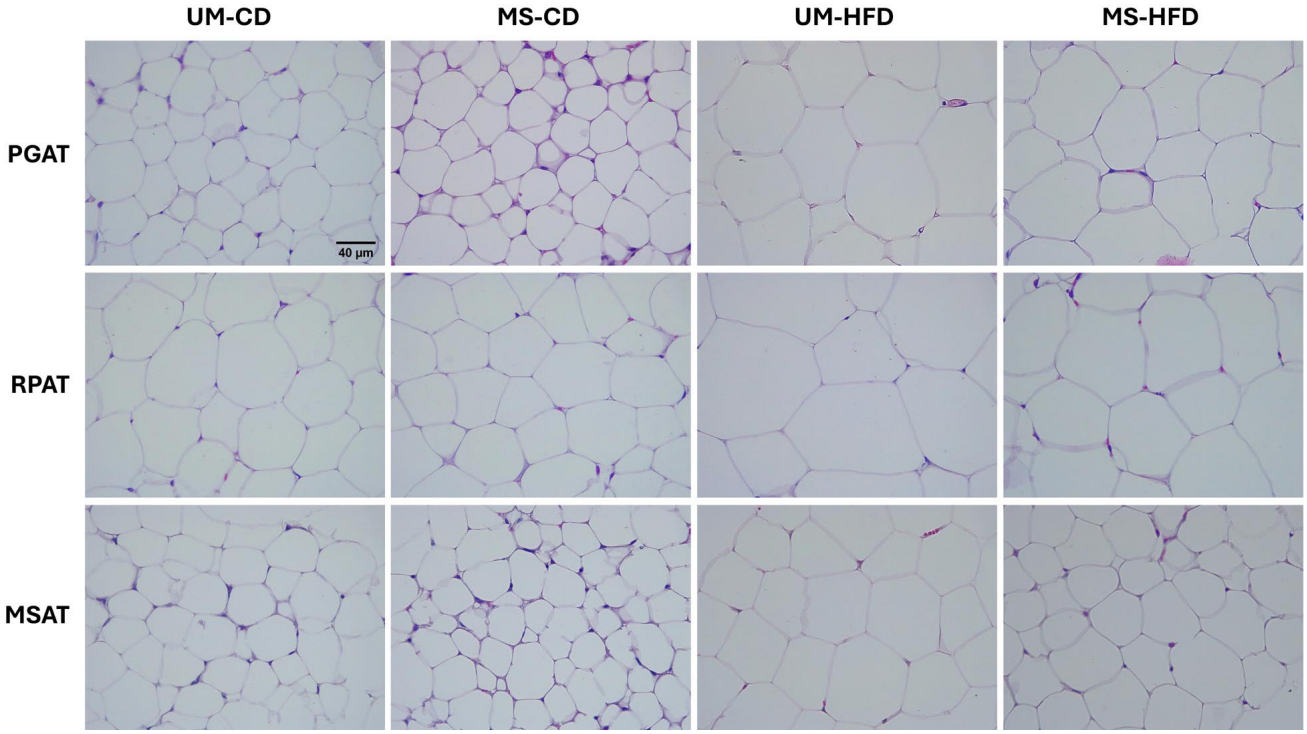

Fig. 6. Representative histological sections of visceral fat pads from male C57BL/6 mice subjected to maternal separation and post-weaning high-fat diet exposure. PGAT: perigonadal fat pad; RPAT: retroperitoneal fat pad; MSAT: mesenteric fat pad. UM-CD: unmanipulated, control diet; MS-CD: maternal separation, control diet; UM-HFD: unmanipulated, high-fat diet; MS-HFD: maternal separation, high-fat diet. Sections were stained with H&E.

Comparison of photomicrographs across the experimental groups revealed progressive changes in adipocyte size, associated with the dietary regimen and modulated by MS. In the groups fed CD (UM-CD and MS-CD), the microscopic fields were dominated by adipocytes of smaller apparent diameter, characterized by greater heterogeneity in cell size within the same field.

In contrast, animals fed HFD (UM-HFD and MS-HFD) exhibited clear alterations in adipose tissue morphology. In the UM-HFD group, the analyzed fields displayed a marked predominance of adipocytes with large apparent diameters, broad cell profiles, well-defined contours, and relatively homogeneous morphology. In these fields, cell size variability was reduced, and adipocytes occupied most of the tissue, producing a pattern dominated by large cells. Similarly, in the MS-HFD group, adipocytes of large apparent size were also observed; however, the distribution of cell diameters was visually more heterogeneous than in the UM-HFD group. In these fields, large adipocytes coexisted with others of intermediate size, resulting in greater morphological variability within the same fat pad. This heterogeneity was particularly evident when comparing equivalent fields between the two HFD groups.

The consistent presence of these morphological differences in the photomicrographs necessitated a quantitative approach to objectively characterize adipocyte size variations between the experimental groups.

Sectional area of adipocytes

SA analysis of adipocytes showed that the dietary regimen was the principal determinant of adipocyte size in all three pads evaluated, while the effect of MS depended on the adipose tissue type (Fig. 7, Table V). This indicates that diet-induced adipocyte expansion is not uniform but varies among the different fat pads analyzed.

Table V. Two-way ANOVA assessing the relative contribution of post-weaning diet, maternal separation (MS), and their interaction (diet × MS) to the variance in mean adipocyte sectional area (SA) within distinct fat pads of male C57BL/6 mice.

Data	Variation and significance test					
	Diet effect		MS effect		Diet x MS	
	%	*p*	%	*p*	%	*p*
PGAT	84.9	<0.0001	1.7	ns	2.6	ns
RPAT	70.1	<0.0001	7.5	0.0018	13.9	0.0001
MSAT	78.3	<0.0001	0.03	ns	4	ns

Perigonadal (PGAT), retroperitoneal (RPAT) and mesenteric (MSAT) adipose tissue deposits. Data represent the percentage of variance explained (%) and the associated p values for each main factor and their interaction. ns: not significant; $p < 0.05$ considered statistically significant.

In PGAT, HFD was associated with a significant increase in SA, independent of MS, suggesting that this fat pad is highly sensitive to dietary challenge. In contrast, MS did not alter adipocyte size under control diet conditions, nor did it significantly potentiate the response to an HFD.

RPAT exhibited the largest absolute adipocyte size among the pads analyzed and a particularly marked response to HFD. In this tissue, beyond the predominant effect of diet, MS contributed significantly, with a diet-MS interaction observed. This suggests that this fat pad is especially susceptible to the convergence of early life programming and postnatal nutritional overload.

MSAT, in contrast, exhibited the lowest SA values and the smallest relative increase with HFD, indicating a more limited capacity for adipocyte expansion compared to the other fat pads. In this tissue, MS was not associated with significant changes in cell size, reinforcing the concept of functional heterogeneity among adipose compartments.

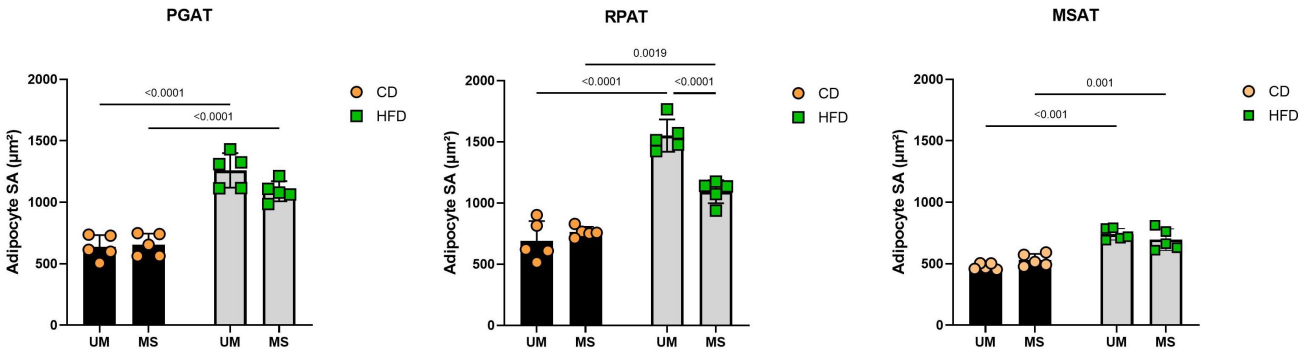

Fig. 7. Sectional area (SA) of adipocytes in male C57BL/6 mice subjected to maternal separation and post-weaning high-fat diet exposure. Perigonadal (PGAT), retroperitoneal (RPAT) and mesenteric (MSAT) adipose tissue deposits; UM: unmanipulated group; MS: maternal separation group; CD: control diet; HFD: high-fat diet. Bar graphs depict mean ± SD; dots indicate individual animals. p-values represent statistically significant differences between groups, determined by two-way ANOVA.

Taken together, the three fat pads demonstrated a hierarchical organization of adipocyte size (RPAT > PGAT > MSAT), and HFD-induced expansion that, while consistent, was not homogeneous across tissues. These findings underscore the importance of the anatomical context of adipose tissue in determining the morphological response to diet and early life programming factors.

To explore whether the expansion of adipose pads was related to changes in adipocyte size, the association between tissue mass and adipocyte size was evaluated (Fig. 8). A positive relationship was observed in all three pads, indicating that an increase in adipose mass is accompanied, to varying extents, by an increase in cell size.

In PGAT, the strong association between fat pad mass and SA suggests that variations in tissue mass are largely explained by changes in adipocyte size. In RPAT, although adipocytes exhibited the highest absolute SA values among the pads, the relationship between fat pad mass and adipocyte size was weaker. This indicates that variations in RPAT mass do not depend exclusively on increased cell size but rather reflect a less proportional relationship between these two parameters.

In MSAT, the more moderate association indicates a relatively minor contribution of adipocyte size to the increase in fat pad mass.

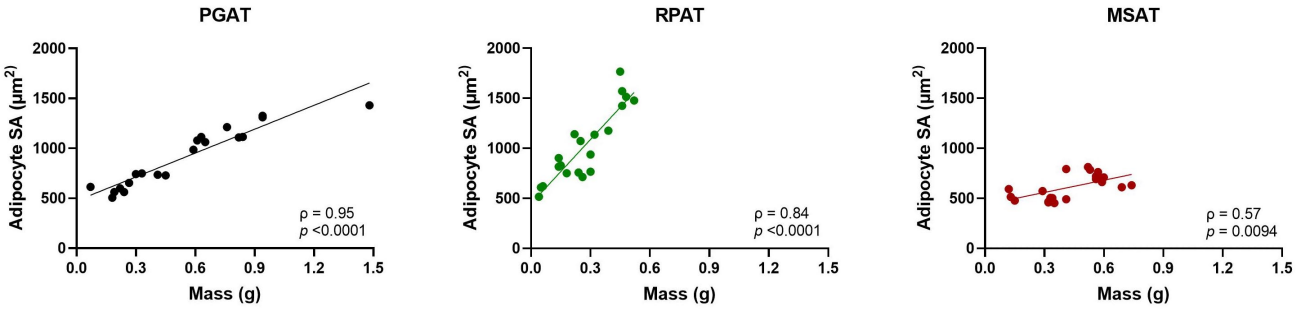

Fig. 8. Correlation between total fat pad mass and mean adipocyte sectional area (SA) in male C57BL/6 mice. Perigonadal (PGAT), retroperitoneal (RPAT) and mesenteric (MSAT) adipose tissue deposits. Scatter plots depict individual animals, with solid lines representing regression fits for visualization. Associations were evaluated using Spearman's rank correlation. Spearman's correlation coefficients (ρ) and p-values are indicated within each panel. n = 20 animals.

DISCUSSION

A high-fat diet is the principal determinant of dyslipidemia, while maternal separation selectively modulates metabolic susceptibility.

Analysis of the plasma lipid profile shows that HFD and MS do not induce a uniform, global dyslipidemia but instead selectively modulate specific lipid fractions, with a predominant impact on cholesterol metabolism and dissociated TG responses. This pattern is consistent with the double-hit model and the literature on early metabolic programming, which indicate that adverse exposures during early stages condition metabolic vulnerability to subsequent challenges (Maniam *et al*., 2014; Eberle *et al*., 2021; Ibayashi & Tsukamoto, 2024).

CHOL-T levels increased in response to both HFD and MS, reaching maximal values when both factors were present. However, the absence of a statistically significant interaction suggests that both stimuli contribute additively, rather than synergistically, to the increased systemic cholesterol burden. This observation is consistent with studies describing persistent alterations in cholesterol metabolism induced by early stress, even under CD, as well as with the established impact of HFD on hepatic cholesterol homeostasis, synthesis, and biliary excretion (Eberle *et al*., 2021; Heeren & Scheja, 2021). In this context, MS may establish a baseline state of metabolic susceptibility upon which HFD acts as a second destabilizing stimulus, in line with previous findings in the same experimental model at the hepatic level (del Sol *et al*., 2025).

In contrast, TG levels showed no significant changes associated with either HFD or MS. This relative stability suggests that, in this model, TG metabolism is regulated by compensatory mechanisms that buffer the impact of excess energy intake and early stress. Given that plasma TG levels reflect a dynamic equilibrium between hepatic VLDL-C secretion, intravascular hydrolysis mediated by lipoprotein lipase, and peripheral fatty acid uptake, it is plausible that adipose tissue expansion acts as an efficient metabolic sink, preventing the development of overt hypertriglyceridemia despite the obesogenic environment (Sylvers-Davie & Davies, 2021; Spitler *et al*., 2021; Gugliucci, 2024).

The behavior of LDL-C provided key information regarding the interaction between early programming and diet. Unlike CHOL-T, LDL-C exhibited a significant interaction between HFD and MS, with a particularly pronounced increase in the MS-HFD group. This observation is consistent with evidence that early stress can induce lasting alterations in hepatic LDL regulation, including reduced plasma clearance mediated by the LDL receptor and qualitative changes in lipoprotein particles (Chechi *et al*., 2009; Maniam *et al*., 2014). Furthermore, the convergence of unfavorable early programming and HFD may promote a pro-inflammatory and oxidative environment that favors a more atherogenic lipoprotein profile, including a greater predominance of small, dense LDL particles (Superko & Garrett, 2022; Bekbossynova *et al*., 2025).

HDL-C exhibited a clearly context-dependent behavior. Under CD, MS was associated with higher HDL-C levels; however, this effect was attenuated under HFD, resulting incomparable levels between the obesogenic diet groups. This pattern reinforces the concept that high-fat diets disrupt HDL homeostasis and reverse cholesterol transport, particularly in the presence of chronic inflammation and metabolic dysfunction (Zhang *et al*., 2019; Stadler *et al*., 2021). In this context, circulating HDL-C levels do not necessarily reflect functional capacity, as HDL's cholesterol efflux ability and anti-inflammatory properties may be compromised even in the absence of apparent quantitative changes (Navab *et al*., 2001; Rohatgi *et al*., 2014; Robert *et al*., 2016).

Taken together, these results indicate that HFD is the principal determinant of the observed dyslipidemia, while MS selectively modulates the magnitude and pattern of the response, especially in the fractions associated with cholesterol metabolism. The dissociation between cholesterol and TG suggests that the metabolic adaptations induced by early programming and nutritional challenge are not manifested as global plasma alterations but rather are directed toward tissue-level lipid partitioning and handling mechanisms.

The global adiposity index predominantly reflects the impact of dietary challenge, with modulation dependent on a history of early-life stress.

The global adiposity index was clearly dominated by dietary regimen, accounting for most of the observed variation, whereas MS did not exert a significant main effect. This finding is consistent with theoretical models of body fat regulation, in which the post-weaning diet serves as the primary modulator of energy balance, while early feeding patterns exert a more subtle influence on adipose tissue distribution and quality (Gesta *et al*., 2007; Speakman *et al*., 2011).

Several studies have shown that MS and other forms of early-life stress preferentially modulate specific fat pads and expansion strategies (hypertrophy *versus* hyperplasia) rather than total body fat (Lecoutre & Breton, 2015). In this context, the absence of differences in the global index does not preclude a significant metabolic impact of MS; rather, it suggests that its effects manifest at regional and structural levels.

The expansion of visceral fat pads is fat pad-specific and reveals a hierarchical organization in the response to diet and early-life stress.

Analysis of visceral fat pad mass revealed pronounced regional heterogeneity in response to HFD and MS. Although overall body mass gain was positively associated with increased PGAT, RPAT, and MSAT mass, differences in regression intercepts indicate distinct baseline masses among fat pads, consistent with fat pad-specific set points and allometric adipose growth (Ibrahim, 2010; DeClercq *et al*., 2016).

In PGAT, expansion was predominantly driven by HFD, with no significant effects attributable to MS or to the interaction between the two factors. This finding supports the notion that PGAT is highly sensitive to post-weaning caloric excess and is relatively less influenced by early adverse experiences when total fat pad mass is assessed (Tchoukalova *et al*., 2010; Jeffery *et al*., 2015).

In contrast, RPAT exhibited a response that was clearly dependent on the interaction between HFD and MS, indicating that this fat pad is particularly sensitive to the convergence of early-life programming and nutritional overload. The high proportion of variance explained by this interaction suggests that early-life history decisively determines the capacity of RPAT to expand in response to energy excess.

MSAT displayed an intermediate pattern, with a dominant effect of diet and a significant interaction with MS. Owing to its anatomical location and portal drainage, this fat pad has particular metabolic relevance, as it directly exposes the liver to free fatty acids and pro-inflammatory mediators, reinforcing its role in adipose-hepatic communication (Rytka *et al*., 2011).

Histological remodeling of adipose tissue reveals heterogeneous expansion mechanisms, with variable

contributions from adipocyte hypertrophy depending on the fat pad location.

Histological analysis showed that HFD induced morphological changes consistent with adipocyte hypertrophy in all three fat pads, with varying magnitudes depending on location. Quantitative analysis of adipocyte SA confirmed that diet was the main determinant of cell size, whereas the contribution of MS depended on the fat pad.

In the PGAT group, HFD significantly increased adipocyte SA independently of MS, suggesting a high sensitivity of this fat pad to caloric excess. In the RPAT group, in addition to the dominant effect of diet, MS contributed significantly, with a diet-MS interaction observed, indicating that this fat pad is particularly susceptible to the convergence of early-life programming and nutritional challenge. Meanwhile, the MSAT group showed the lowest SA values and the smallest relative increase with HFD, suggesting a more limited adipocyte expansion capacity.

Considered together, the fat pads showed a consistent hierarchy in adipocyte size (RPAT > PGAT > MSAT) and HFD-induced expansion that, although widespread, was not homogeneous. The positive correlation between fat pad mass and adipocyte SA indicates that hypertrophy contributes significantly to tissue expansion, although with a less proportional relationship in RPAT and MSAT, suggesting the additional involvement of other mechanisms, such as hyperplasia and tissue remodeling (Spalding *et al*., 2008; Jo *et al*., 2009; Sun *et al*., 2011; Wu *et al*., 2017).

Limitations and projections

Among the principal limitations of this study is the exclusive use of male mice, which restricts the extrapolation of findings to females, where early-life programming and stress responses may differ substantially. Additionally, the absence of molecular and functional analyses precludes a deeper understanding of the mechanisms underlying the observed differences between fat pads. These limitations are inherent to morphological studies and underscore the need for future integrative approaches that incorporate both sexes, molecular analyses, and functional assessments of adipose tissue and systemic metabolism (Mandarim-de-Lacerda *et al*., 2021; Börgeson *et al*., 2022).

CONCLUSIONS

This study demonstrates that, in a murine model of early-life stress induced by MS and post-weaning HFD exposure, the observed metabolic and morphological alterations arise from a dynamic interaction between early-life history and the subsequent nutritional environment.

HFD was identified as the principal determinant of disruption to the plasma lipid profile, while MS acted as a modulator, selectively enhancing certain alterations induced by the nutritional challenge. This pattern supports the notion that early-life programming does not define the metabolic phenotype in isolation but rather conditions the response to subsequent stimuli.

Accordingly, the expansion of visceral adipose tissue was fat pad-dependent, without a uniform overall increase in adiposity. MS differentially modulated the response of specific fat pads to diet, demonstrating a hierarchical functional organization of adipose tissue. Histologically, this expansion was associated with fat pad-dependent structural remodeling, with variable contributions from adipocyte hypertrophy, suggesting heterogeneous cellular mechanisms of tissue growth.

Taken together, these findings indicate that MS is not a direct determinant of obesity, but rather a reprogramming factor that modulates the response of visceral adipose tissue and lipid metabolism to an adverse nutritional environment in adulthood, highlighting the role of early-life context in the functional organization of the adipose-metabolic axis.

NAVARRETE, J. & VÁSQUEZ, B. Efectos de la separación materna sobre la homeostasis lipídica y la organización del tejido adiposo visceral en ratones alimentados con dieta alta en grasas post-destete. *Int. J. Morphol., 44(1)*:9-22, 2026.

RESUMEN: El estrés temprano y la obesidad representan desafíos críticos para la salud pública. Este estudio evaluó el impacto de la separación materna (MS), como modelo de adversidad temprana, y el consumo de una dieta alta en grasas (HFD) post-destete sobre el perfil lipídico y la organización del tejido adiposo visceral en ratones C57BL/6. Ratones machos fueron sometidos a MS durante la vida postnatal temprana o se mantuvieron sin manipular (UM). Después del destete, los animales fueron asignados a una dieta de control (CD) o una HFD, formando cuatro grupos (n = 5 por grupo): UM-CD, SM-CD, UM-HFD y SM-HFD. Se evaluó el perfil lipídico plasmático, el índice global de adiposidad, la masa de los depósitos adiposos viscerales perigonadal (PGAT), retroperitoneal (RPAT) y mesentérico (MSAT), así como la arquitectura histológica y el área seccional (SA) de los adipocitos mediante análisis morfológicos y cuantitativos. La HFD se identificó como el principal determinante de las alteraciones del perfil lipídico plasmático, particularmente del CHOL-T y LDL-C, mientras que la MS moduló selectivamente la magnitud de estas alteraciones. El índice global de adiposidad estuvo dominado por el efecto dietario, sin diferencias atribuibles a la MS. En contraste, la expansión de los depósitos adiposos viscerales fue heterogénea y dependiente del compartimento,

observándose una interacción significativa dieta-SM en el RPAT y, en menor medida, en el MSAT. A nivel histológico y cuantitativo, la HFD indujo un aumento significativo del SA adipocitario en los tres depósitos viscerales, con una contribución moduladora de la MS dependiente del tejido, evidenciando patrones de expansión adiposa no uniformes. En conclusión, estos hallazgos indican que la MS no actúa como un determinante directo de obesidad, sino como un factor de programación que modula el perfil lipídico plasmático y la respuesta estructural del tejido adiposo visceral frente a un entorno nutricional obesogénico en la adultez.

PALABRAS CLAVE: Separación materna; Dieta alta en grasas; Perfíl lipídico; Tejido adiposo visceral; Ratón.

REFERENCIAS

Aguila, M. B.; Ornellas, F. & Mandarim-de-Lacerda, C. A. Nutritional research and fetal programming: parental nutrition influences the structure and function of the organs. *Int. J. Morphol., 39(1)*:327-34, 2021.

Barouki, R.; Gluckman, P. D.; Grandjean, P.; Hanson, M. & Heindel, J. J. Developmental origins of non-communicable disease: Implications for research and public health. *Environ Health, 11*:42, 2012.

Bekbossynova, M.; Saliev, T.; Ivanova-Razumova, T.; Andossova, S.; Kali, A. & Myrzakhmetova, G. Small dense LDL: An underestimated driver of atherosclerosis (Review). *Mol. Med. Rep., 32(6)*:328, 2025.

Börgeson, E.; Boucher, J. & Hagberg, C. E. Of mice and men: Pinpointing species differences in adipose tissue biology. *Front. Cell Dev. Biol., 10*:1003118, 2022.

Canadian Council on Animal Care. *Guide to the Care and Use of Experimental Animals*. 2nd ed., Vol. 1. Canadian Council on Animal Care, Ottawa, 1993. Available online: https://ccac.ca/Documents/Standards/Guidelines/Guide_to_the_Care_and_Use_of_Experimental_Animals_Vol1.pdf

Chechi, K.; McGuire, J. J. & Cheema, S. K. Developmental programming of lipid metabolism and aortic vascular function in C57BL/6 mice: a novel study suggesting an involvement of LDL-receptor. *Am. J. Physiol. Regul. Integr. Comp. Physiol., 296(4)*:R1029-R1040, 2009.

Choe, S. S.; Huh, J. Y.; Hwang, I. J.; Kim, J. I. & Kim, J. B. Adipose tissue remodeling: Its role in energy metabolism and metabolic disorders. *Front. Endocrinol. (Lausanne), 7*:30, 2016.

Cruz-Orive, L. M. & Weibel, E. R. Recent stereological methods for cell biology: a brief survey. *Am. J. Physiol. Lung Cell Mol. Physiol., 258(4)*:L148-L156, 1990.

Daskalakis, N. P.; Oitzl, M. S.; Schächinger, H.; Champagne, D. L. & Ronald de Kloet, E. Testing the cumulative stress and mismatch hypotheses of psychopathology in a rat model of early-life adversity. *Physiol. Behav., 106(5)*:707-21, 2012.

DeClercq, V. C.; Goldsby, J. S.; McMurray, D. N. & Chapkin, R. S. Distinct adipose depots from mice differentially respond to a high-fat, high-salt diet123. *J. Nutr., 146(6)*:1189-96, 2016.

del Sol, M.; Navarrete, J.; García-Orozco, L.; Duque-Colorado, J.; Sócola-Barsallo, Z.; Sandoval, C. & Vásquez, B. When timing matters: effects of maternal separation and post-weaning high-fat diet on liver morphology in a rodent model. *Nutrients, 17(10)*:1619, 2025.

Di Cesare, M.; Soric´, M.; Bovet, P.; Miranda, J. J.; Bhutta, Z.; Stevens, G. A.; Laxmaiah, A.; Kengne, A.-P. & Bentham, J. The epidemiological burden of obesity in childhood: a worldwide epidemic requiring urgent action. *BMC Med., 17*:212, 2019.

Eberle, C.; Fasig, T.; Brüseke, F. & Stichling, S. Impact of maternal prenatal stress by glucocorticoids on metabolic and cardiovascular outcomes in their offspring: A systematic scoping review. *PLOS ONE, 16(1)*:e0245386, 2021.

George, E. D.; Bordner, K. A.; Elwafi, H. M. & Simen, A. A. Maternal separation with early weaning: a novel mouse model of early life neglect. *BMC Neurosci., 11*:123, 2010.

Gesta, S.; Tseng, Y.-H. & Kahn, C.R. Developmental origin of fat: tracking obesity to its source. *Cell, 131(2)*:242-56, 2007.

Gluckman, P. D.; Hanson, M. A. & Pinal, C. The developmental origins of adult disease. *Matern. Child. Nutr., 1(3)*:130-41, 2005.

Gugliucci, A. Angiopoietin-like proteins and lipoprotein lipase: The waltz partners that govern triglyceride-rich lipoprotein metabolism? impact on atherogenesis, dietary interventions, and emerging therapies. *J. Clin. Med., 13(17)*:5229, 2024.

Gundersen, H. J. G.; Jensen, E. B. V.; Kiêu, K. & Nielsen, J. The efficiency of systematic sampling in stereology - reconsidered. *J. Microsc., 193(Pt 3)*:199-211, 1999.

Guzik, T. J.; Skiba, D. S.; Touyz, R. M. & Harrison, D. G. The role of infiltrating immune cells in dysfunctional adipose tissue. *Cardiovasc. Res., 113(9)*:1009-23, 2017.

Heeren, J. & Scheja, L. Metabolic-associated fatty liver disease and lipoprotein metabolism. *Mol. Metab., 50*:101238, 2021.

Holtrup, B.; Church, C. D.; Berry, R.; Colman, L.; Jeffery, E.; Bober, J. & Rodeheffer, M. S. Puberty is an important developmental period for the establishment of adipose tissue mass and metabolic homeostasis. *Adipocyte, 6(3)*:224-33, 2017.

Ibayashi, M. & Tsukamoto, S. Lipid remodelling in mammalian development. *Nat. Cell Biol., 26(2)*:179-80, 2024.

Ibrahim, M. M. Subcutaneous and visceral adipose tissue: structural and functional differences. *Obes. Rev., 11(1)*:11-8, 2010.

Jeffery, E.; Church, C. D.; Holtrup, B.; Colman, L. & Rodeheffer, M. S. Rapid depot-specific activation of adipocyte precursor cells at the onset of obesity. *Nat. Cell Biol., 17(4)*:376-85, 2015.

Jo, J.; Gavrilova, O.; Pack, S.; Jou, W.; Mullen, S.; Sumner, A. E.; Cushman, S. W. & Periwal, V. Hypertrophy and/or hyperplasia: dynamics of adipose tissue growth. *PLoS Comput. Biol., 5(3)*:e1000324, 2009.

Kirichenko, T. V.; Markina, Y. V.; Bogatyreva, A. I.; Tolstik, T. V.; Varaeva, Y. R.; Starodubova, A. V. The role of adipokines in inflammatory mechanisms of obesity. *Int. J. Mol. Sci., 23(23)*:14982, 2022.

Kwon, H. & Pessin, J. E. Adipokines mediate inflammation and insulin resistance. *Front. Endocrinol. (Lausanne), 4*:71, 2013.

Leachman, J. R.; Cincinelli, C.; Ahmed, N.; Dalmasso, C.; Xu, M.; Gatineau, E.; Nikolajczyk, B. S.; Yiannikouris, F.; Hinds, T. D. & Loria, A. S. Early life stress exacerbates obesity in adult female mice via mineralocorticoid receptor-dependent increases in adipocyte triglyceride and glycerol content. *Life Sci., 304*:120718, 2022.

Lecoutre, S. & Breton, C. Maternal nutritional manipulations program adipose tissue dysfunction in offspring. *Front. Physiol., 6*:158, 2015.

López, C. B.; Moreno, G. G. & Palloni, A. Empirical evidence of predictive adaptive response in humans: a meta- analysis of migrant populations. *J. Dev. Orig. Health Dis., 14(6)*:728-45, 2023.

López-Taboada, I.; Arboleya, S.; Sal-Sarria, S.; Gueimonde, M.; González-Pardo, H. & Conejo, N. M. Combined effects of early life stress and prolonged exposure to western diet on emotional responses and gut microbiota. *Psicothema, 36(2)*:133-44, 2024.

Mandarim-de-Lacerda, C. A.; del Sol, M. Tips for studies with quantitative morphology (Morphometry and Stereology). *Int. J. Morphol., 35(4)*:1482-94, 2017.

Mandarim-de-Lacerda, C. A.; del Sol, M.; Vásquez, B. & Aguila, M. B. Mice as an animal model for the study of adipose tissue and obesity. *Int. J. Morphol., 39(6)*:1521-8, 2021.

Maniam, J.; Antoniadis, C. & Morris, M. J. Early-life stress, HPA axis adaptation, and mechanisms contributing to later health outcomes. *Front. Endocrinol. (Lausanne), 5*:73, 2014.

Morton, D. B. & Griffiths, P. H. Guidelines on the recognition of pain, distress and discomfort in experimental animals and an hypothesis for assessment. *Vet. Rec., 116(16)*:431-6, 1985.

Institute for Laboratory Animal Research. *Guide for the Care and Use of Laboratory Animals*; National Academies Press, Washington, DC, USA, 2011.

Navab, M.; Berliner, J. A.; Subbanagounder, G.; Hama, S.; Lusis, A. J.; Castellani, L.W.; Reddy, S.; Shih, D.; Shi, W.; Watson, A. D.; Van Lenten, B. J.; Vora, D. & Fogelman, A. M. HDL and the inflammatory response induced by LDL-derived oxidized phospholipids. *Arterioscler. Thromb. Vasc. Biol., 21(4)*:481-8, 2001.

Nishi, M. Effects of early-life stress on the brain and behaviors: implications of early maternal separation in rodents. *Int. J. Mol. Sci., 21(19)*:7212, 2020.

Radzik-Zaja¸c, J.; Wytrychowski, K.; Wis´niewski, A. & Barg, W. The role of the novel adipokines vaspin and omentin in chronic inflammatory diseases. *Pediatr. Endocrinol. Diabetes Metab., 29(1)*:48-52, 2023.

Rees, S. L.; Akbari, E.; Steiner, M. & Fleming, A. S. Effects of early deprivation and maternal separation on pup-directed behavior and HPA axis measures in the juvenile female rat. *Dev. Psychobiol., 50(4)*:315-321, 2008.

Reeves, P. G.; Nielsen, F. H. & Fahey, G. C. AIN-93 purified diets for laboratory rodents: final report of the American Institute of Nutrition ad hoc writing committee on the reformulation of the AIN-76A rodent diet. *J. Nutr., 123(11)*:1939-51, 1993.

Robert, S.; Brewer, H. B.; Ansell, B. J.; Barter, P.; Chapman, M. J.; Heinecke, J. W.; Kontush, A.; Tall, A. R.; & Webb, N. R. Dysfunctional HDL and atherosclerotic cardiovascular disease. *Nat. Rev. Cardiol., 13(1)*:48-60, 2016.

Rodríguez-González, G. L.; Santos, S. D. L.; Méndez-Sánchez, D.; Reyes-Castro, L. A.; Ibáñez, C. A.; Canto, P. & Zambrano, E. High-fat diet consumption by male rat offspring of obese mothers exacerbates adipose tissue hypertrophy and metabolic alterations in adult life. *Br. J. Nutr., 130(5)*:783-92, 2023.

Rohatgi, A.; Khera, A.; Berry, J. D.; Givens, E. G.; Ayers, C. R.; Wedin, K. E.; Neeland, I. J.; Yuhanna, I. S.; Rader, D. R.; de Lemos, J. A. & Shaul, P. W. HDL cholesterol efflux capacity and incident cardiovascular events. *N. Engl. J. Med., 371(25)*:2383-93, 2014.

Russell, W. M. S. & Burch, R. L. *The principles of humane experimental technique*. Universities Federation for Animal Welfare, Wheathampstead, UK, 1959; reprinted in 1992.

Rytka, J. M.; Wueest, S.; Schoenle, E. J. & Konrad, D. The portal theory supported by venous drainage–selective fat transplantation. *Diabetes, 60(1)*:56-63, 2011.

Sakers, A.; De Siqueira, M. K.; Seale, P. & Villanueva, C. J. Adipose-tissue plasticity in health and disease. *Cell, 185(3)*:419-46, 2022.

Saklayen, M. G. The global epidemic of the metabolic syndrome. *Curr. Hypertens. Rep., 20(2)*:12, 2018.

Sheng, J. A.; Bales, N. J.; Myers, S. A.; Bautista, A. I.; Roueinfar, M.; Hale, T. M. & Handa, R. J. The hypothalamic-pituitary-adrenal axis: Development, programming actions of hormones, and maternal-fetal interactions. *Front. Behav. Neurosci., 14*:601939, 2021.

Silva, M. C.; Galindo, L. C. M.; Souza, J. A.; Castro, R. M.; & Souza, S. L. Perinatal stress: characteristics and effects on adult eating behavior. *Rev. Nutr., 26(4)*:473-80, 2013.

Slomianka, L. & West, M. J. Estimators of the precision of stereological estimates: An example based on the CA1 pyramidal cell layer of rats. *Neuroscience, 136(3)*:757-67, 2005.

Spalding, K. L.; Arner, E.; Westermark, P. O.; Bernard, S.; Buchholz, B. A.; Bergmann, O.; Blomqvist, L.; Hoffstedt, J.; Näslund, E.; Britton, T.; Concha, H.; Hassan, M.; Rydén, M.; Frisén, J. & Arner, P. Dynamics of fat cell turnover in humans. *Nature, 453(7196)*:783-7, 2008.

Speakman, J. R.; Levitsky, D. A.; Allison, D. B.; Bray, M. S.; de Castro, J. M.; Clegg, D. J.; Clapham, J. C.; Dulloo, A. G.; Gruer, L.; Haw, S.; Hebebrand, J.; Hetherington, M. M.; Higgs, S.; Jebb, S. A.; Loos, R. J. F.; Luckman, S.; Luke, A.; Mohammed-Ali, V.; O'Rahilly, S.; Pereira, M.; Perusse, L.; Robinson, T. N.; Rolls, B.; Symonds, M. E. & Westerterp-Plantenga, M. S. Set points, settling points and some alternative models: theoretical options to understand how genes and environments combine to regulate body adiposity. *Dis. Model. Mech., 4(6)*:733-45, 2011.

Spitler, K. M.; Shetty, S. K.; Cushing, E. M.; Sylvers-Davie, K. L. & Davies, B. S. J. Regulation of plasma triglyceride partitioning by adipose-derived ANGPTL4 in mice. *Sci. Rep., 11(1)*:7873, 2021.

Stadler, J. T.; Lackner, S.; Mörkl, S.; Trakaki, A.; Scharnagl, H.; Borenich, A.; Wonisch, W.; Mangge, H.; Zelzer, S.; Meier-Allard, N.; Holasek, S.J.; & Marsche, G. Obesity affects HDL metabolism, composition and subclass distribution. *Biomedicines, 9(3)*:242, 2021.

Sun, K.; Kusminski, C. M. & Scherer, P.E. Adipose tissue remodeling and obesity. *J. Clin. Invest., 121(6)*:2094-101, 2011.

Superko, H. & Garrett, B. Small dense LDL: Scientific background, clinical relevance, and recent evidence still a risk even with 'normal' LDL-C Levels. *Biomedicines, 10(4)*:829, 2022.

Sylvers-Davie, K. L. & Davies, B. S. J. Regulation of lipoprotein metabolism by ANGPTL3, ANGPTL4, and ANGPTL8. *Am. J. Physiol. Endocrinol. Metab., 321(4)*:E493-E508, 2021.

Tamashiro, K. L. K.; Terrillion, C. E.; Hyun, J.; Koenig, J. I. & Moran, T. H. Prenatal stress or high-fat diet increases susceptibility to diet-induced obesity in rat offspring. *Diabetes, 58(5)*:1116-25, 2009.

Tchoukalova, Y. D.; Votruba, S. B.; Tchkonia, T.; Giorgadze, N.; Kirkland, J. L. & Jensen, M. D. Regional differences in cellular mechanisms of adipose tissue gain with overfeeding. *Proc. Natl. Acad. Sci. U S A, 107(42)*:18226-31, 2010.

Vargas, J.; Junco, M.; Gomez, C. & Lajud, N. Early life stress increases metabolic risk, HPA axis reactivity, and depressive-like behavior when combined with postweaning social isolation in rats. *PLOS ONE, 11(9)*:e0162665, 2016.

Vickers, M. H. Early life nutrition, epigenetics and programming of later life disease. *Nutrients, 6(6)*:2165-78, 2014.

Wolterink-Donselaar, I. G.; Meerding, J. M. & Fernandes, C. A method for gender determination in newborn dark pigmented mice. *Lab. Anim., 38(1)*:35-8, 2009.

Wu, Y.; Lee, M.-J.; Ido, Y. & Fried, S. K. High-fat diet-induced obesity regulates MMP3 to modulate depot- and sex-dependent adipose expansion in C57BL/6J mice. *Am. J. Physiol. Endocrinol. Metab., 312(1)*:E58-E71, 2017.

Yang, H.; Chen, N.; Fan, L.; Lin, X.; Liu, J.; You, Y.; Zhong, Y.; Chen, Y.; Li, J. & Xiao, X. Pre-weaning exposure to maternal high-fat diet is a critical developmental window for programming the metabolic system of offspring in mice. *Front. Endocrinol. (Lausanne), 13*:816107, 2022.

Zatterale, F.; Longo, M.; Naderi, J.; Raciti, G. A.; Desiderio, A.; Miele, C. & Beguinot, F. Chronic adipose tissue inflammation linking obesity to insulin resistance and type 2 diabetes. *Front. Physiol., 10*:1607, 2020.

Zhang, T.; Chen, J.; Tang, X.; Luo, Q.; Xu, D. & Yu, B. Interaction between adipocytes and high-density lipoprotein:new insights into the mechanism of obesity-induced dyslipidemia and atherosclerosis. *Lipids Health Dis., 18(1)*:223, 2019.

Zimmerberg, B. & Sageser, K. A. Comparison of two rodent models of maternal separation on juvenile social behavior. *Front. Psychiatry, 2*:39, 2011.

Corresponding author:
Bélgica Vásquez
Doctoral Program in Morphological Sciences
Faculty of Medicine
Universidad de La Frontera
Temuco
CHILE

E-mail: belgica.vasquez@ufrontera.cl

Bélgica Vásquez https://orcid.org/0000-0002-4106-3548
Javiera Navarrete https://orcid.org/0009-0008-5347-4820